

Research Article

Effects of Sulfurization Pressure on the Conversion Efficiency of Cosputtered $\text{Cu}_2\text{ZnSnS}_4$ Thin Film Solar Cells

Arun Khalkar,¹ Kwang-Soo Lim,¹ Seong-Man Yu,¹ Dong-Wook Shin,¹
Tae-Sik Oh,² and Ji-Beom Yoo^{1,3}

¹SKKU Advanced Institute of Nanotechnology (SAINT), Sungkyunkwan University, Suwon 440746, Republic of Korea

²Department of Information Display, Sun Moon University, Asan 336708, Republic of Korea

³School of Advanced Materials Science and Engineering, Sungkyunkwan University, Suwon 440746, Republic of Korea

Correspondence should be addressed to Ji-Beom Yoo; jbyoo@skku.edu

Received 2 July 2015; Revised 21 September 2015; Accepted 21 October 2015

Academic Editor: Thomas Unold

Copyright © 2015 Arun Khalkar et al. This is an open access article distributed under the Creative Commons Attribution License, which permits unrestricted use, distribution, and reproduction in any medium, provided the original work is properly cited.

We report herein $\text{Cu}_2\text{ZnSnS}_4$ (CZTS) thin film solar cells with 6.75% conversion efficiency, without an antireflection coating. The CZTS precursors have been prepared by cosputtering using three different targets on Mo-coated substrates: copper (Cu), tin sulfide (SnS), and zinc (Zn). The postsulfurization was carried out at different pressures in a $\text{H}_2\text{S}/\text{N}_2$ environment at 550°C for one hour. A comparative study on the performances of solar cells with CZTS absorber layers prepared at different sulfurization pressures was carried out. The device efficiency of 1.67% using CZTS absorber and low pressure sulfurization is drastically improved, to an efficiency of 6.75% with atmospheric pressure sulfurization.

1. Introduction

Photovoltaic (PV) technology using heterojunction thin film solar cells has remarkable potential to generate renewable energy. Meanwhile, several fabrication techniques have been adopted to prepare high performance thin film solar cells by using abundant materials. The absorber layer for the thin film solar cells can be prepared by various methods like sputtering, evaporation, electrodeposition, sol gel techniques, and spray pyrolysis [1–11], using abundant materials such as kesterite $\text{Cu}_2\text{ZnSnS}_4$ (CZTS) [2], Cu_2SnS_3 [12], Cu_2S [13], SnS [14], Zn_3P_2 [15], and hybrid perovskite $\text{CH}_3\text{NH}_3\text{PbI}_3$ [16–18]. In particular, the sputtering deposition technique has the advantages of easy control and tuning of the material composition of the film. CZTS has been receiving noticeable attention because of its nontoxic and abundant constituent elements. Solar cells using CZTS absorber layers prepared by postsulfurization of a coevaporated metal sulfur precursor layer showed a certified efficiency of 8.4% [2]. Scragg et al. prepared CZTS precursors by reactively cosputtering in a pure H_2S atmosphere and showed 7.9% efficiency by 570°C sulfurization for 10 min in sulfur vapor [19]. Also Tajima et al.

reported 8.8% efficiency using a two-layered CZTS absorber prepared by sputtering [20]. The fabrication route based on sputtering technology with postsulfurization demonstrates the more promising results. It should be noted that the technology based on sputtering stands out from the other chemical methods as having the promise of lending itself to large-scale industrial manufacturing. The feasibility of optimizing the postsulfurization process is another important factor that determines whether or not a CZTS solar cell of high efficiency can be produced. The parameters in the sulfurization process, such as the chemistry of the chosen atmosphere, the temperature profile with time, and the pressure, are linked to each other and can affect the crystallization process with regard to elemental composition variance, grain boundaries, and grain size. To grow the CZTS absorber layer, the sulfurization process can be done either at low temperature for a long time (500–530°C for 1–2 hours) or at high temperature for a short time (550–580°C for 5–20 min). An H_2S gas annealing atmosphere can form large-grained CZTS films with uniform diffusion of the elements [21]. It is important to explore the sulfurization process with due regard to the optimization of the annealing parameters

in order to produce CZTS solar cells with high conversion efficiencies. CZTS has a small parameter window within which to bring about a thermodynamically stable phase [22]. A very small variation in the sulfurization parameters favors the formation of secondary phases such as Cu_2SnS_3 , ZnS , SnS_2 , and Cu_2S and consequently CZTS films have been investigated extensively with regard to the source of the sulfur [23, 24], sulfurization time [25, 26], sulfurization temperature [27, 28], and sulfur partial pressure [29, 30]. However, few reports are available on the effect of pressure during sulfurization, which has an important influence on the quality of CZTS film and also affects the formation of a MoS_2 layer at the interface between the CZTS and Mo.

In this work, we report the comparison of morphological, compositional, and structural properties of the CZTS thin films sulfurized at different pressures and the corresponding device performance. The CZTS films were deposited by cosputtering on Mo-coated soda lime glass (SLG) using Cu, SnS, and Zn targets, followed by postsulfurization in H_2S gas atmosphere at 550°C for one hour at different sulfurization pressures. The solar cell devices were fabricated using a CZTS absorber layer with the sequence of SLG/Mo/CZTS/CdS/i-ZnO/Al:ZnO/Ni-Al. The cell device performance was characterized by current-voltage (I - V) measurements and external quantum efficiency (EQE). A detailed explanation of Raman and XRD peaks corresponding to the CZTS kesterite phase is also presented.

2. Experimental Details

The precursor layer for the CZTS absorber was deposited on a molybdenum- (Mo-) coated glass substrate by cosputtering of three two-inch-diameter sputter targets—Cu (99.9%), SnS (99.9%), and Zn (99.9%)—respectively, connected to DC, RF1, and RF2 power supplies. The details of magnetron sputtering system are given elsewhere [4, 5]. The Mo-coated glass was cleaned by acetone, methanol, and DI water before the deposition of the CZTS absorber layer. The target powers of 15, 35, and 80 W were used for the Cu, SnS, and Zn targets, respectively. The film was deposited for 40 min with a working pressure of 1 mT. This was followed by an annealing of the CZTS layer in $\text{N}_2/\text{H}_2\text{S}$ (95/5%) mixed gas environment at 550°C for 1 hour in a furnace, inside a quartz tube. Prior to sulfurization at 550°C , soft annealing (S.A.) at 350°C for 30 min was carried out in the same environment at atmospheric pressure to prevent evaporation and loss of elements. The sulfurization was performed at different pressures. The sulfurization pressure inside the quartz tube was maintained at 780, 760, 730, 700, and 670 Torr by passing mixed gas at the flow rate of 50 SCCM. The detailed sulfurization procedure is explained in Supplementary Information and is shown in Figure S1, available online at <http://dx.doi.org/10.1155/2015/750846>. The surface and cross-sectional morphologies of the film were characterized by a scanning electron microscope (SEM; JSM7401F, JEOL). The phase purity of the CZTS layer was assessed by high resolution X-ray diffraction (XRD; D8 Discover, Bruker) and Raman scattering spectroscopy with excitation wavelength of 532 nm. The elemental composition of the film was confirmed

by X-ray fluorescence spectrometry (XRF; Primus 2, Rigaku). The solar cell device was fabricated by deposition of an n-type CdS buffer layer which was synthesized using chemical bath deposition. Before deposition of the CdS layer, the CZTS surface was etched for five minutes in a 0.5 M potassium cyanide (KCN) solution prepared in DI water. Then a transparent conductive oxide (TCO) layer of i-ZnO/Al:ZnO was deposited by RF-magnetron sputtering. The device was then completed by thermal evaporation and deposition of a Ni/Al upper electrode grid. The thicknesses of the CdS, i-ZnO, and Al:ZnO layers were around 60 nm, 50 nm, and 450 nm, respectively. The measurements of current-voltage (I - V) characteristics were performed for solar cells fabricated with CZTS layers prepared in different sulfurization pressures under AM 1.5G one-sun illumination ($100\text{ mW}/\text{cm}^2$) using a solar simulator (Oriel Sol 3A class AAA). The quantum efficiency measurement was carried out using a commercial photovoltaic measurements system (PV Measurement Inc., Boulder, CO) with a 75 W xenon lamp (Ushio, Japan) as a light source in DC mode.

3. Results and Discussion

The surface and cross-sectional SEM images of the CZTS films prepared by cosputtering and sulfurized at various sulfurization pressures are shown in Figure 1. The measured film thickness of all samples is approximately $1.0\text{ }\mu\text{m}$. As shown in Figure 1(a), the sample prepared at 780 Torr sulfurization pressure shows big grains with few voids on the surface of the film. The cross-sectional image of the same sample shows compact and void-free morphology. The sample sulfurized at a pressure of one atmosphere (760 Torr) shows large, uniform grains with well-defined grain boundaries and a faceted surface of compact cross section extending through the thickness of the film, as shown in Figure 1(b). It is important to obtain a CZTS absorber layer with a morphology that consists of well-defined grain boundaries which act as less recombination sites for electrons [31]. As the sulfurization pressure decreased from 730 to 670 Torr, the grain size became bigger and finally a few big grains broke down into small grains. The surface and cross-sectional images of the films are shown in Figures 1(c)–1(e). At low pressures, the melting point of metal sulfides decreases during the sulfurization process and so liquid Cu_2S may help to increase the grain size [32]. Also, due to different diffusion coefficients of the elements the Kirkendall effect can be observed during low pressure sulfurization. That brings about the formation of voids and secondary phases like SnS, Cu_2S , or ZnS [33, 34].

The elemental composition of the sulfurized CZTS films has been characterized by XRF. The observed atomic percentage and atomic ratios of Cu, Zn, Sn, and S are shown in Table 1. The film prepared at 780 Torr sulfurization pressure shows Cu-rich and Zn-poor composition which can lead to the formation of a Cu_2S secondary phase. The films were soft annealed at 350°C for 30 min at atmospheric pressure which helped prevent evaporation and loss of elements. All the samples show atomic % and the ratios close to the desired range as reported for high-efficiency CZTS solar cells [1, 2].

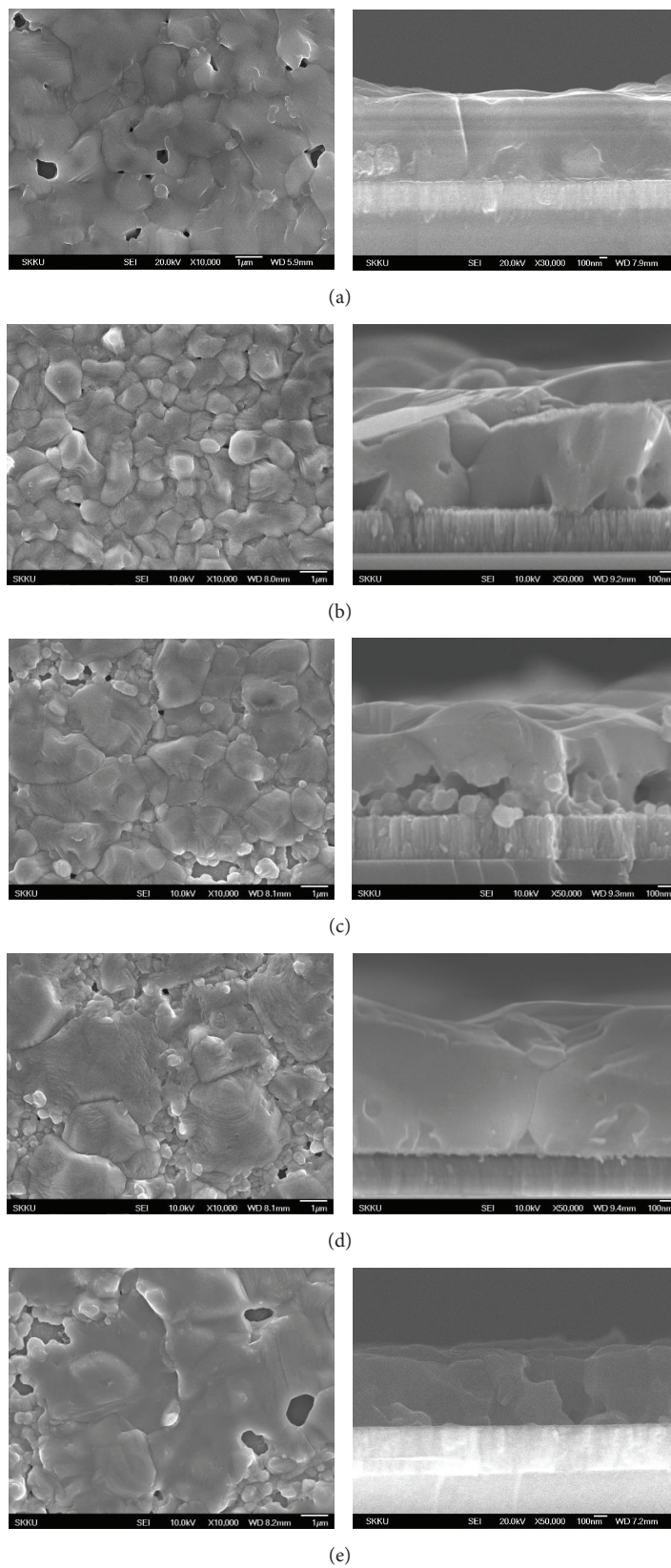


FIGURE 1: Surface (left) and cross section (right) SEM images of CZTS thin films sulfurized at (a) 780 Torr, (b) 760 Torr, (c) 730 Torr, (d) 700 Torr, and (e) 670 Torr in H_2S gas atmosphere at 550°C .

TABLE 1: Elemental composition of the sulfurized CZTS thin films by XRF.

Elements	Atomic %				
	780 Torr	760 Torr	730 Torr	700 Torr	670 Torr
Cu	21.14	21.00	20.72	20.85	21.00
Zn	13.23	14.53	14.84	14.86	14.90
Sn	11.45	12.05	12.56	12.44	12.76
S	54.16	52.40	51.81	51.82	51.34
Zn/Sn	1.15	1.20	1.10	1.20	1.15
Cu/(Zn + Sn)	0.85	0.78	0.75	0.76	0.75
S/(Cu + Zn + Sn)	1.18	1.10	1.07	1.07	1.05

Raman scattering with a 532 nm excitation wavelength has been employed to confirm CZTS phase formation and to detect the presence of secondary phases, as shown in Figure 2. All the films exhibit a major peak at 336 cm^{-1} which is identified as the main vibrational A1 symmetry mode, along with one weak peak at 284 cm^{-1} [4, 5]. Raman spectra also reveal the presence of Cu_2S with a characteristic mode at 476 cm^{-1} in the film that was sulfurized at higher than atmospheric pressure, at 780 Torr. Raman spectra also reveal the presence of MoS_2 with characteristic modes at 408 cm^{-1} and 380 cm^{-1} in the films sulfurized at 730, 700, and 670 Torr. Only the pure CZTS phase was identified in the film sulfurized at atmospheric pressure.

The crystallinity and the orientation of the films were investigated using X-ray diffraction (XRD), as shown in Figure 3. All of the films show main peaks at 2θ values of 28.5, 32.9, 47.3, 56.1, and 76.4 degrees, respectively, corresponding to (112), (200), (220), (312), and (332) planes in the tetragonal body-centered kesterite CZTS phase—according to JCPDS card number 26-0575. The XRD pattern also shows the Mo peaks at 2θ values of 40.5, 58.5, and 73.6 degrees, respectively, corresponding to (110), (200), and (211) planes in body-centered cubic Mo—according to JCPDS card number 04-0809. The XRD results show excellent agreement with the previously reported results and confirm that the CZTS thin films were formed with good crystallinity [4, 5]. The secondary phase peaks were observed at a 2θ value of 31.77 degrees, which corresponds to the Cu_2S phase, and 26.65 degrees, which corresponds to the SnS phase—for the films sulfurized at higher (780 Torr) and lower (670 Torr) pressures, respectively. The formation of Cu_2S and SnS secondary phases results in an interfacial recombination due to the lattice mismatch with CZTS and a decrease in open-circuit voltage due to the different energy band gap [35, 36]. The formation of MoS_2 at the interface between Mo and CZTS was detected in the films sulfurized at lower pressure. The MoS_2 layer may be helpful as an electrical quasiohmic contact and can improve the adhesion between CZTS and Mo back contact but it can also lead to a high series resistance if it is not thin enough [37].

The current density voltage (J - V) curves for solar cells were measured under AM1.5 and 100 mW/cm^2 illumination and the detailed photovoltaic properties are shown in Figure 4 and summarized in Table 2. The device fabricated

TABLE 2: Photovoltaic properties of the CZTS solar cells.

Sulfurization pressure (Torr)	J_{sc} (mA/cm^2)	V_{oc} (Volt)	FF	$\eta\%$
780	11.0	0.520	0.5506	3.15
760	16.75	0.630	0.6398	6.75
730	14.20	0.610	0.5425	4.70
700	10.62	0.557	0.5578	3.30
670	7.00	0.425	0.5445	1.62

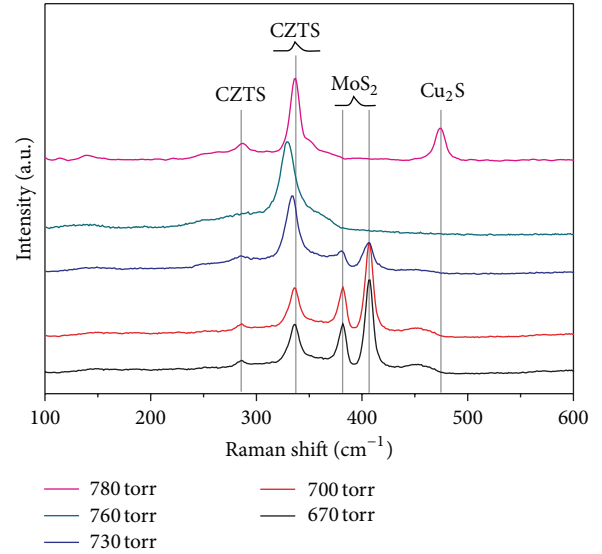


FIGURE 2: Raman spectra of sulfurized CZTS films.

with the CZTS absorber formed at a 760 Torr sulfurization pressure shows 6.75% efficiency. The improvement in the efficiency comes from the enhancement of V_{oc} . As the sulfurization pressure decreases from 730 Torr to 670 Torr, the efficiency of the devices decreases from 4.70% to 1.62%. The deterioration in photovoltaic properties mainly comes from nonuniform CZTS grain size and the presence of voids which leads to low V_{oc} and FF. The degradation in J_{sc} and V_{oc} that was observed for the device with the CZTS absorber formed at the sulfurization pressure of 780 Torr may be mainly due to the presence of the Cu_2S phase. The solar cell efficiency with the CZTS deposited by cosputtering showed 6.77% by Katagiri et al. [1]. Similarly efficiencies of 6.3% and 9.2% have been reported by Solar Frontier for CZTS with CdS and for hybrid (CdS + InS) n-type layers, respectively [38]. The conversion efficiency of 6.75% reported here is for the cell without antireflection (AR) coating.

Figure 5 shows the external quantum efficiency (EQE) spectra of all solar cells for the wavelength range between 200 and 1000 nm. The device fabricated with the CZTS absorber formed at 760 Torr sulfurization pressure shows higher EQE values, indicating improved carrier collection which may be due to the larger junction area and less absorption by CdS. The curve gradually decreases in the long wavelength area suggesting a shorter carrier diffusion length and lower collection efficiency in the bulk of CZTS absorber. The J_{sc} of

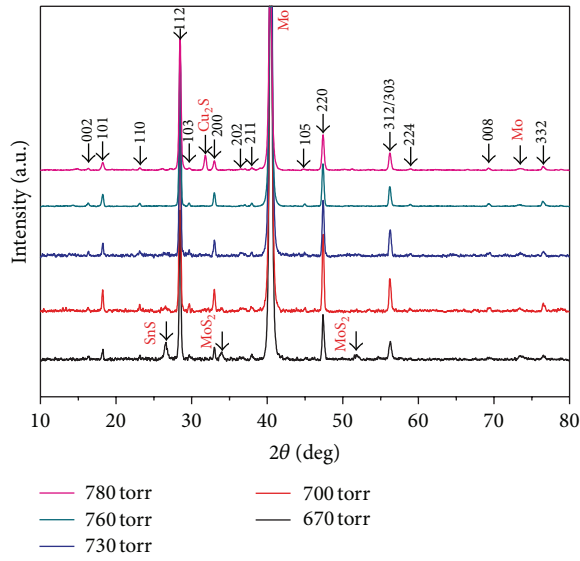


FIGURE 3: XRD spectra of sulfurized CZTS films.

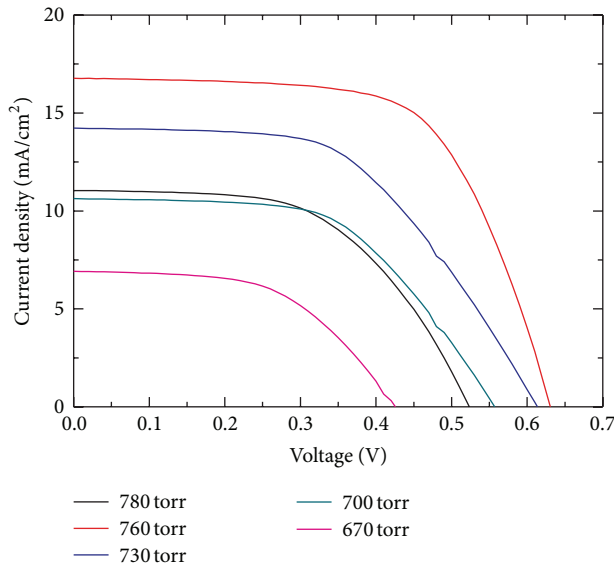


FIGURE 4: Current-voltage curves of the CZTS solar cells.

16.56 mA/cm² was recorded for the same CZTS device. The short circuit current values obtained from both EQE and *J*-*V* tests are almost the same. Similarly, as the sulfurization pressure decreases from 730 Torr to 670 Torr, the EQE of the devices decreases. To improve the CZTS device efficiency and *J*_{sc}, further CdS and transparent conductive oxide (TCO) optimization is required. The approaches for minimizing broadband reflection and maximizing total transmission into the CZTS absorbing layer require a different device architecture compared to that which serves mainly to minimize reflection [39].

4. Conclusion

A 6.75% efficient CZTS solar cell was fabricated using cosputtering followed by sulfurization in H₂S gas at atmospheric

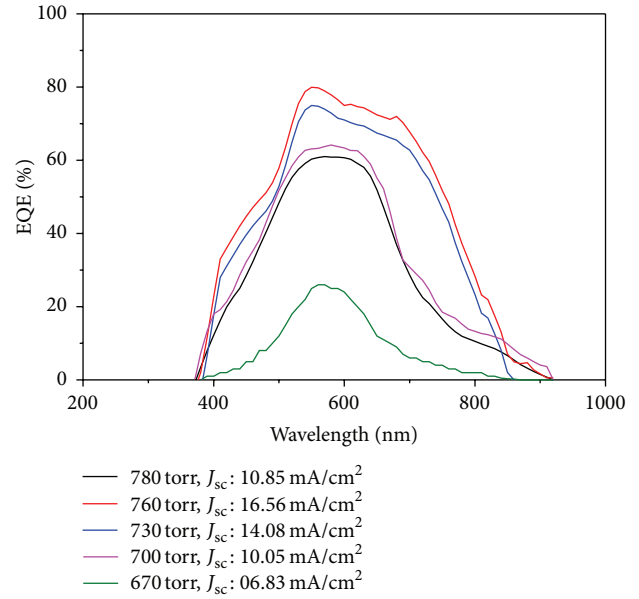


FIGURE 5: External quantum efficiency (EQE) curves of the CZTS solar cells.

pressure. The solar cell shows a higher EQE value, particularly in the blue light wavelength region, due to the larger junction area. A solar cell with CZTS formed at atmospheric pressure shows significant enhancement in *V*_{oc} and FF compared to CZTS prepared at low sulfurization pressure under 730 Torr. The formation under low pressure sulfurization of MoS₂ at the back contact and nonuniform grains with big voids leads to low *J*_{sc} and *V*_{oc}. The Cu₂S phase was found in film prepared at 780 Torr, which impaired the CZTS solar cell performance. To improve the CZTS device performance, optimization of sulfurization strategies in order to bring about good CZTS absorber morphology is required. Furthermore, CdS and TCO layer optimization is needed to enhance the photoreponse throughout the solar spectral range.

Conflict of Interests

The authors declare that there is no conflict of interests regarding the publication of this paper.

Acknowledgment

This work was supported by the "Global Leading Technology Program" of the Office of Strategic R&D Planning (OSP), funded by the Ministry of Knowledge Economy, Republic of Korea (no. S-2012-1226-000).

References

- [1] H. Katagiri, K. Jimbo, S. Yamada et al., "Enhanced conversion efficiencies of Cu₂ZnSnS₄-based thin film solar cells by using preferential etching technique," *Applied Physics Express*, vol. 1, no. 4, Article ID 041201, 2 pages, 2008.

- [2] B. Shin, O. Gunawan, Y. Zhu, N. A. Bojarczuk, S. J. Chey, and S. Guha, "Thin film solar cell with 8.4% power conversion efficiency using an earth-abundant $\text{Cu}_2\text{ZnSnS}_4$ absorber," *Progress in Photovoltaics: Research and Applications*, vol. 21, no. 1, pp. 72–76, 2013.
- [3] K. Wang, O. Gunawan, T. Todorov et al., "Thermally evaporated $\text{Cu}_2\text{ZnSnS}_4$ solar cells," *Applied Physics Letters*, vol. 97, no. 14, Article ID 143508, 2010.
- [4] A. Khalkar, K.-S. Lim, S.-M. Yu, S. P. Patole, and J.-B. Yoo, "Deposition of $\text{Cu}_2\text{ZnSnS}_4$ thin films by magnetron sputtering and subsequent sulphurization," *Electronic Materials Letters*, vol. 10, no. 1, pp. 43–49, 2014.
- [5] A. Khalkar, K.-S. Lim, S.-M. Yu, S. P. Patole, and J.-B. Yoo, "Effect of growth parameters and annealing atmosphere on the properties of $\text{Cu}_2\text{ZnSnS}_4$ thin films deposited by cosputtering," *International Journal of Photoenergy*, vol. 2013, Article ID 690165, 7 pages, 2013.
- [6] A. Weber, H. Krauth, S. Perlt et al., "Multi-stage evaporation of $\text{Cu}_2\text{ZnSnS}_4$ thin films," *Thin Solid Films*, vol. 517, no. 7, pp. 2524–2526, 2009.
- [7] A. Ennaoui, M. Lux-Steiner, A. Weber et al., " $\text{Cu}_2\text{ZnSnS}_4$ thin film solar cells from electroplated precursors: novel low-cost perspective," *Thin Solid Films*, vol. 517, no. 7, pp. 2511–2514, 2009.
- [8] K. Tanaka, M. Oonuki, N. Moritake, and H. Uchiki, " $\text{Cu}_2\text{ZnSnS}_4$ thin film solar cells prepared by non-vacuum processing," *Solar Energy Materials and Solar Cells*, vol. 93, no. 5, pp. 583–587, 2009.
- [9] N. Kamoun, H. Bouzouita, and B. Rezig, "Fabrication and characterization of $\text{Cu}_2\text{ZnSnS}_4$ thin films deposited by spray pyrolysis technique," *Thin Solid Films*, vol. 515, no. 15, pp. 5949–5952, 2007.
- [10] D. B. Mitzi, O. Gunawan, T. K. Todorov, K. Wang, and S. Guha, "The path towards a high-performance solution-processed kesterite solar cell," *Solar Energy Materials and Solar Cells*, vol. 95, no. 6, pp. 1421–1436, 2011.
- [11] H. Katagiri, " $\text{Cu}_2\text{ZnSnS}_4$ thin film solar cells," *Thin Solid Films*, vol. 480–481, pp. 426–432, 2005.
- [12] U. Mitsutaro, T. Yasuhiko, M. Tomoyoshi, S. Takenobu, A. Hiroki, and M. Ryosuke, " $\text{Cu}_2\text{Sn}_{1-x}\text{Ge}_x\text{S}_3$ ($x = 0.17$) thin-film solar cells with high conversion efficiency of 6.0%," *Applied Physics Express*, vol. 6, no. 4, Article ID 045501, 2013.
- [13] S. C. Riha, S. Jin, S. V. Baryshev, E. Thimsen, G. P. Wiederrecht, and A. B. F. Martinson, "Stabilizing Cu_2S for photovoltaics one atomic layer at a time," *ACS Applied Materials and Interfaces*, vol. 5, no. 20, pp. 10302–10309, 2013.
- [14] P. Sinsermsuksakul, L. Sun, S. W. Lee et al., "Overcoming efficiency limitations of Sns-based solar cells," *Advanced Energy Materials*, vol. 4, no. 15, Article ID 41400496, 2014.
- [15] O. Vazquez-Mena, J. P. Bosco, O. Ergen et al., "Performance enhancement of a graphene-zinc phosphide solar cell using the electric field-effect," *Nano Letters*, vol. 14, no. 8, pp. 4280–4285, 2014.
- [16] J. Cui, F. Meng, H. Zhang et al., " $\text{CH}_3\text{NH}_3\text{PbI}_3$ -based planar solar cells with magnetron-sputtered nickel oxide," *ACS Applied Materials & Interfaces*, vol. 6, no. 24, pp. 22862–22870, 2014.
- [17] J. Shi, Y. Luo, H. Wei et al., "Modified two-step deposition method for high-efficiency $\text{TiO}_2/\text{CH}_3\text{NH}_3\text{PbI}_3$ heterojunction solar cells," *ACS Applied Materials and Interfaces*, vol. 6, no. 12, pp. 9711–9718, 2014.
- [18] J. Xiao, Y. Yang, X. Xu et al., "Pressure-assisted $\text{CH}_3\text{NH}_3\text{PbI}_3$ morphology reconstruction to improve the high performance of perovskite solar cells," *Journal of Materials Chemistry A*, vol. 3, no. 10, pp. 5289–5293, 2015.
- [19] J. J. Scragg, T. Kubart, J. T. Wätjen, T. Ericson, M. K. Linnarsson, and C. Platzer-Björkman, "Effects of back contact instability on $\text{Cu}_2\text{ZnSnS}_4$ devices and processes," *Chemistry of Materials*, vol. 25, no. 15, pp. 3162–3171, 2013.
- [20] S. Tajima, T. Itoh, H. Hazama, K. Ohishi, and R. Asahi, "Improvement of the open-circuit voltage of $\text{Cu}_2\text{ZnSnS}_4$ cells using a two-layered process," in *Proceedings of the 40th IEEE Photovoltaic Specialist Conference (PVSC '14)*, pp. 431–434, IEEE, Denver, Colo, USA, June 2014.
- [21] A. Khalkar, K.-S. Lim, S.-M. Yu, J. H. Kim, and J.-B. Yoo, "Sulfurization approach using sulfur vapor, graphite box and H_2S gas atmospheres for co-sputtered $\text{Cu}_2\text{ZnSnS}_4$ thin film," in *Proceedings of the 40th IEEE Photovoltaic Specialist Conference (PVSC '14)*, pp. 0390–0394, Denver, Colo, USA, June 2014.
- [22] A. Nagoya, R. Asahi, R. Wahl, and G. Kresse, "Defect formation and phase stability of $\text{Cu}_2\text{ZnSnS}_4$ photovoltaic material," *Physical Review B*, vol. 81, no. 11, Article ID 113202, 2010.
- [23] G. Brammertz, M. Buffière, S. Oueslati et al., "Characterization of defects in 9.7% efficient $\text{Cu}_2\text{ZnSnSe}_4$ -CdS-ZnO solar cells," *Applied Physics Letters*, vol. 103, no. 16, Article ID 163904, 2013.
- [24] S. M. Pawar, A. I. Inamdar, B. S. Pawar et al., "Synthesis of $\text{Cu}_2\text{ZnSnS}_4$ (CZTS) absorber by rapid thermal processing (RTP) sulfurization of stacked metallic precursor films for solar cell applications," *Materials Letters*, vol. 118, pp. 76–79, 2014.
- [25] H. Guan, H. Shen, C. Gao, and X. He, "Sulfurization time effects on the growth of $\text{Cu}_2\text{ZnSnS}_4$ thin films by solution method," *Journal of Materials Science: Materials in Electronics*, vol. 24, no. 8, pp. 2667–2671, 2013.
- [26] P. A. Fernandes, P. M. P. Salomé, A. F. Sartori et al., "Effects of sulphurization time on $\text{Cu}_2\text{ZnSnS}_4$ absorbers and thin films solar cells obtained from metallic precursors," *Solar Energy Materials and Solar Cells*, vol. 115, pp. 157–165, 2013.
- [27] A. Emrani, P. Vasekar, and C. R. Westgate, "Effects of sulfurization temperature on CZTS thin film solar cell performances," *Solar Energy*, vol. 98, pp. 335–340, 2013.
- [28] K. Maeda, K. Tanaka, Y. Nakano, and H. Uchiki, "Annealing temperature dependence of properties of $\text{Cu}_2\text{ZnSnS}_4$ thin films prepared by sol-gel sulfurization method," *Japanese Journal of Applied Physics*, vol. 50, no. 5, Article ID 05FB08, 2011.
- [29] B.-A. Schubert, B. Marsen, S. Cinque et al., " $\text{Cu}_2\text{ZnSnS}_4$ thin film solar cells by fast coevaporation," *Progress in Photovoltaics: Research and Applications*, vol. 19, no. 1, pp. 93–96, 2011.
- [30] J. J. Scragg, J. T. Wätjen, M. Edoff, T. Ericson, T. Kubart, and C. Platzer-Björkman, "A detrimental reaction at the molybdenum back contact in $\text{Cu}_2\text{ZnSn}(\text{S},\text{Se})_4$ thin-film solar cells," *Journal of the American Chemical Society*, vol. 134, no. 47, pp. 19330–19333, 2012.
- [31] J. B. Li, V. Chawla, and B. M. Clemens, "Investigating the role of grain boundaries in CZTS and CZTSSe thin film solar cells with scanning probe microscopy," *Advanced Materials*, vol. 24, no. 6, pp. 720–723, 2012.
- [32] I. Repins, C. Beall, N. Vora et al., "Co-evaporated $\text{Cu}_2\text{ZnSnSe}_4$ films and devices," *Solar Energy Materials and Solar Cells*, vol. 101, pp. 154–159, 2012.
- [33] J. J. Scragg, *Copper Zinc Tin Sulfide Thin Films for Photovoltaics*, Springer, Berlin, Germany, 2011.
- [34] K. Zeng, R. Stierman, T.-C. Chiu, D. Edwards, K. Ano, and K. N. Tu, "Kirkendall void formation in eutectic SnPb solder joints on bare Cu and its effect on joint reliability," *Journal of Applied Physics*, vol. 97, no. 2, Article ID 024508, 2005.

- [35] S. Sohila, M. Rajalakshmi, C. Ghosh, A. K. Arora, and C. Muthamizhchelvan, "Optical and Raman scattering studies on SnS nanoparticles," *Journal of Alloys and Compounds*, vol. 509, no. 19, pp. 5843–5847, 2011.
- [36] B. G. Mendis, M. C. J. Goodman, J. D. Major, A. A. Taylor, K. Durose, and D. P. Halliday, "The role of secondary phase precipitation on grain boundary electrical activity in $\text{Cu}_2\text{ZnSnS}_4$ (CZTS) photovoltaic absorber layer material," *Journal of Applied Physics*, vol. 112, no. 12, Article ID 124508, 2012.
- [37] B. Shin, N. A. Bojarczuk, and S. Guha, "On the kinetics of MoSe_2 interfacial layer formation in chalcogen-based thin film solar cells with a molybdenum back contact," *Applied Physics Letters*, vol. 102, no. 9, Article ID 091907, 2013.
- [38] H. Hiroi, N. Sakai, T. Kato, and H. Sugimoto, "High voltage $\text{Cu}_2\text{ZnSnS}_4$ submodules by hybrid buffer layer," in *Proceedings of the 39th IEEE Photovoltaic Specialists Conference (PVSC '13)*, pp. 863–866, Tampa, Fla, USA, June 2013.
- [39] M. T. Winkler, W. Wang, O. Gunawan, H. J. Hovel, T. K. Todorov, and D. B. Mitzi, "Optical designs that improve the efficiency of $\text{Cu}_2\text{ZnSn}(\text{S,Se})_4$ solar cells," *Energy and Environmental Science*, vol. 7, no. 3, pp. 1029–1036, 2014.

